Solar Phys (2017) 292:142
DOI 10.1007/s11207-017-1166-4

Understanding Problem Forecasts of ISEST Campaign Flare-CME Events

David Webb[1] · **Nariaki Nitta**[2]

Received: 17 February 2017 / Accepted: 5 September 2017

Abstract The goal of the International Study of Earth-affecting Solar Transients (ISEST) project as part of the Variability of the Sun and Its Terrestrial Impact (VarSITI) program is to understand the origin, evolution, and propagation of solar transients through the space between the Sun and Earth, and to improve our prediction capability for space weather. A goal of ISEST Working Group 4 (Campaign Events) is to study a set of well-observed Sun-to-Earth events to develop an understanding of why some events are successfully forecast (textbook cases), whereas others become problem or failed forecasts. In this article we study six cases during the rise of Solar Cycle 24 that highlight forecasting problems. Likely source coronal mass ejections (CMEs) were identified in all six cases, but the related solar surface activity ranged from uncertain or weak to X-class flares. The geoeffects ranged from none to severe as in the two Sun–Earth events in 2015 that caused severe storms. These events were chosen to illustrate some key problems in understanding the chain from cause to geoeffect.

Keywords Forecasting · Space weather · Coronal mass ejections

1. Introduction

1.1. Background

Solar transients, mainly coronal mass ejections (CMEs), flares, and corotating interaction regions (CIRs), are important aspects of coronal and interplanetary dynamics. CMEs are the dominant short-term contributor because they inject large quantities of mass and magnetic

Earth-affecting Solar Transients
Guest Editors: Jie Zhang, Xochitl Blanco-Cano, Nariaki Nitta, and Nandita Srivastava

✉ D. Webb
david.webb@bc.edu

1 ISR, Boston College, 140 Commonwealth Ave., Chestnut Hill, MA 02659, USA

2 Lockheed Martin Solar and Astrophysics Laboratory, 3251 Hanover Street, Palo Alto, CA 94304, USA

Published online: 22 September 2017

flux into the heliosphere, causing major transient disturbances. CMEs can drive interplanetary shocks, which are a key source of solar energetic particles (SEPs). CMEs and their associated phenomena have the most severe space weather consequences at Earth. The effects of these transients on our society include deleterious impacts on satellite operations, radio communication problems, enhanced radiation risks for aircraft crew and passengers, and outages and damage to electric power networks on the ground.

In the past there have been many studies attempting to link solar activity and CMEs observed near the Sun with their interplanetary counterparts, *i.e.* ICMEs, usually observed *in situ* at 1 AU. These include studies of applied space weather, wherein attempts are made to forecast the geoeffectiveness of transients, or to try to understand "problem" events for which the forecasts fail in some sense. Schwenn (2006) provides a good earlier review of CMEs, ICMEs, and space weather. More recent prediction or probability studies involving large numbers of CMEs and/or ICMEs include Zhang *et al.* (2007), Rodriguez *et al.* (2009), Möstl *et al.* (2014), and Dumbović *et al.* (2015). In the past decade or so, the use of white-light imagers on the *Solar Mass Ejection Imager* (SMEI) and the *Heliospheric Imagers* (HIs) on the *Solar-Terrestrial Relations Observatory* (STEREO) have helped to bridge the gap between coronagraph observations near the Sun and *in situ* measurements at 1 AU, and thus to track especially CMEs through the inner heliosphere to Earth. Space weather studies involving large numbers of CMEs include Webb *et al.* (2009) using SMEI data and Möstl *et al.* (2014) with STEREO/HI data.

A current international community effort addressing how solar variability affects Earth is the five-year (2014 – 2018) Scientific Committee on Solar-Terrestrial Physics (SCOSTEP) program, called Variability of the Sun and Its Terrestrial Impact (VarSITI). VarSITI focuses on the period of the low solar activity Cycle 24 and its consequences at Earth. The International Study of Earth-affecting Solar Transients (ISEST) is one of four VarSITI projects. Its goals are to (1) understand the origin, evolution, and propagation of solar transients (CMEs, flares, CIRs) through the heliosphere between the Sun and Earth, and (2) improve the prediction capability for the arrival of these transients and their potential impacts at Earth (*i.e.* space weather).

These ISEST goals are enabled by continuous observations of Sun and heliosphere from an array of spacecraft and ground-based instruments, global numerical simulations of the system, and theoretical analyses. The issues faced for research and improving the prediction capability include the transit times of CMEs and shocks from the Sun to their arrival at Earth and their impacts or geoeffects. The degree of geoeffectiveness is determined by various parameters, such as arrival speed, magnetic field orientation (*e.g.*, B_Z in the geocentric solar ecliptic (GSE) system), and the complexity of the ambient solar wind.

To study all the issues and place the results in a global picture, the ISEST project consists of seven working groups (WGs), covering data analysis, theoretical interpretations, modeling, and campaign event study. The ISEST leaders have created a Wiki site for data repository, discussions, and education: http://solar.gmu.edu/heliophysics/index.php/Main_Page.

ISEST Working Group 4 focuses on the study of campaign events and is led by the authors of this article. The task of WG 4 is to integrate theory, simulations, and observations to better understand the chain of cause-effect activity from the Sun to Earth for a few carefully selected events. ISEST provides "textbook", or well-understood, Sun to Earth cases to the community, but WG 4 also examines more controversial events, such as stealth CMEs and problem ICMEs, to enhance our understanding. An emphasis of WG 4 is on why forecasts fail and how we can improve our predictions. This includes analyzing the complications in linking CMEs to ICMEs, usually observed only *in situ*.

This article summarizes the WG 4 results that highlight the forecasting problems involved in six case studies. These cases generally included major solar flares and CMEs,

and the geoeffects ranged from none to severe, as in the two Sun–Earth events in 2015 that caused "superstorms". These six cases were chosen to illustrate some key problems in understanding the chain from cause to geoeffect.

1.2. History

We have had several ISEST workshops over the last several years, both stand-alone and in conjunction with other large meetings. The main focus of the early ISEST meetings was on one textbook event, 12 – 14 July 2012, and one problem event, 4 – 8 Oct. 2012. The first ISEST workshop was in June 2013 in Hvar, Croatia. This preceded the VarSITI "kickoff" meeting at the Climate and Weather of the Sun–Earth System II (CAWSES-II) Symposium held in November 2013 in Nagoya, Japan. The event list was then expanded to include more recent Sun–Earth events with interesting challenges. The second ISEST workshop was held after the Solar-Terrestrial Physics 13 (STP-13) Symposium held in October 2014 in Xian, China. WG 4 had a presentation at the Solar Heliospheric and INterplanetary Environment (SHINE) workshop held in July 2015 at Stowe, VT, USA. The third ISEST workshop was held in October 2015 in Mexico City, Mexico, and the fourth was in conjunction with the First VarSITI Workshop held in June 2016 at Albena, Bulgaria.

These workshops have covered data collation and analysis, theoretical interpretations, modeling, and the campaign event studies. The presentations and discussions at these meetings have helped our understanding of the six case studies in this article. A focus of the third and fourth ISEST workshops was on the two severe storms in 2015. Key results from the workshop discussions and the ensuing articles for our six cases are summarized herein. The key WG 4 participants who contributed to the analyses of these cases are listed in the Acknowledgments.

2. Case Studies and Results

2.1. Characteristics of the Case Studies

Table 1 is a summary of the 11 events that have been discussed and analyzed in detail by WG 4. These studies have resulted in many presentations and articles in the literature. The first six events were chosen as VarSITI-wide Campaign Study Events because they had certain space weather effects of interest to one or more of the other three VarSITI projects: Specification and Prediction of the Coupled Inner-Magnetospheric Environment (SPeCIMEN – magnetosphere), Role Of the Sun and the Middle atmosphere/thermosphere/ionosphere In Climate (ROSMIC), and Solar Evolution and Extrema (SEE – solar magnetic records and extreme events). A focus of this article is to understand the Sun-to-Earth cause-effect chain for five of these six campaign events.

The other 5 of the 11 events were chosen because of particular aspects of interest to ISEST WG 4 that help elucidate the Sun-to-Earth chain. One of these five "extra" events, on 10 – 13 September 2014, was of wide interest and is also analyzed in this article.

The six events were selected to illustrate the range of problems that can occur in understanding the complete chain of activity from its source region(s) at the Sun, its propagation through the heliosphere, to its effects at Earth. For each event we note the official NOAA forecast that was issued after each solar event but before its arrival at Earth, and whether the forecast was successful or was problematic in some important manner.

Table 1 ISEST WG4 Event List.

Dates	Source	Response at Earth	Dst	Kp/G level	WG4 type	Forecast success
VarSITI-wide Campaign Study Events						
*1) 12 – 14 July 2012	X1 flare, fast CME	Shock, MC, strong storm	−127	7/G3	T	Underpredicted
*2) 4 – 8 Oct. 2012	Strong CME, but multiple weak surface signatures	Slow propagation to Earth. Moderate storm	−105	6+/G2	P/U	Underpredicted
3) 15 – 17 Mar. 2013	M1 flare, EP, IV, fast halo	Shock, MC?, SEP, strong storm	−132	6+/G2	T	
*4) 1 June 2013	Slow CME on 27 May? CH influence?	Cause of strong storm unclear, CIR?	−119	7/G3	P	Failed-not predicted
*5) 15 – 17 Mar. 2015	C9, C2 flare, EP, fast CME	Shock, sheath, MC, severe storm, FD	−223	8+/G4	P/U	Underpredicted
*6) 21 – 24 June 2015	2 M flares, fast halo CMEs	Shock, sheath, MC, SEP, severe storm	−204	8+/G4	T?	Mostly successful
Other ISEST/MiniMax Study Events						
7) 7 – 9 Mar. 2012	X5 flare, wave, fast CME	Shock, MC, severe storm	−131	8/G4	T	
8) 23 – 24 July 2012	2 flares, EPs	Extreme Stereo-A event, strong storm	Carr.-type	–	T?	
9) 6 Jan. 2012	CME < 2000 km s^{-1}, over solar west limb	GLE at Earth	No	–	P/U	
10) 7 – 9 Jan. 2014	X1 fl, wave, fast asym. halo CH deflection, AR channeling?	Shock, SEP. No storm.	No	≤ 3	P/U	
*11) 10 – 13 Sep. 2014	X2 flare, wave, sym. halo. Source AR evolution of interest.	Shock, MC, moderate Storm, FD	−75	7/G3	P/U	Overpredicted

Source: EP = eruptive prominence, AR = active region, CH = coronal hole; asym. means asymmetrical halo CME and sym. means symmetrical halo CME.

Response at Earth: MC = magnetic cloud, SEP = solar energetic particle event, CIR = corotating interaction region, GLE = ground-level event, FD = Forbush decrease.

Type: T = textbook; U = understand chain; P = problem.

* means an events featured in this article.

For this purpose the forecasts we use were the 3-Day Forecast, the 3-Day Geomagnetic Forecast, and Forecast Discussion as are issued by the NOAA Space Weather Prediction Center (SWPC) on a twice-daily basis. The 3-Day Forecast is "designed to be a one page, simple look at recently observed and a three day forecast of space weather conditions." The 3-Day Geomagnetic Forecast is "a daily deterministic and probabilistic forecast, for the next three days, of geomagnetic activity," and includes estimates of the Ap and Kp geomagnetic indices and what the storm level will be. These are listed in the NOAA Space Weather Scales under five categories of geomagnetic storms, G1 – G5, described as minor, moderate, strong, severe, and extreme: (http://www.swpc.noaa.gov/noaa-scales-explanation). As stated there: "The scales describe the environmental disturbances for three event types: geomagnetic storms, solar radiation storms, and radio blackouts. The scales have numbered levels, analogous to hurricanes, tornadoes, and earthquakes that convey severity. They list possible effects at each level." The G-storm scales are related to the 3-hour Kp index, from 5 – 9, which we use to determine how successful the forecast of geoeffects was. The Forecast Discussion is a brief, but more detailed discussion of the observed data, analysis, and forecast rationale that goes into that 3-day forecast. Summaries of these forecasts are available under Reports of Solar and Geophysical Activity (RSGA) through the SWPC site: ftp://ftp.swpc.noaa.gov/pub/warehouse/.

WG 4 classified the studied events into three general categories. In the first category are possible textbook cases in which the complete chain of a well-observed event is relatively well understood from its solar source, through its heliospheric propagation, to its effects at Earth. These cases involve forecasts that are successful in a general way. Another category includes cases in which there were problems understanding the complete chain, but which we think we now understand. Thus, something was missing in the chain of a well-observed event, but in retrospect after analysis, we now understand why. These cases usually involve forecasts that failed because they were not geoeffective, or were otherwise not accurate. Finally, there are problem cases in which the chain is not complete and we still do not understand why.

2.2. A Possible Textbook Event

On 12 July 2012, an eruptive X1.4 flare occurred, originating from active region (AR) 11520 (S17 W08) with an X-ray peak $\sim$ 16:45 UT. Later during its rotation, the same active region produced several strong flares and CMEs, including the 23 – 24 July CME, which was aimed at the *Solar Terrestrial Relations Observatory* (STEREO) A and was one of the fastest, most energetic CME ever observed (*e.g.* Baker *et al.*, 2013; Liu *et al.*, 2014). The 12 July CME was observed in just a few frames of the coronagraphs of the *Large Angle Spectroscopic Coronagraph* (LASCO) onboard the *Solar and Heliospheric Observatory* because of contamination by solar energetic particles (SEPs). These showed a full-halo CME with an initial speed $\sim 1300\ \mathrm{km\,s^{-1}}$, slightly brighter to the southwest, matching the slightly off-center disk location of the flare (Figure 1, left). On the right side of Figure 1 is an enlarged *Atmospheric Imaging Assembly* (AIA) image showing the source region and dimming. (Note that CME speeds measured from a single viewpoint, such as LASCO, are estimated speeds projected against the plane of the sky. Thus, unless the bulk of the CME mass is at the solar limb, the projected speeds are lower limits to the true speed.) Both of the STEREO heliospheric imagers observed the event, allowing it to be tracked earthward to at least 80 R_S (solar radii) (Hess and Zhang, 2014; Shen *et al.*, 2014; Möstl *et al.*, 2014; Hu *et al.*, 2016).

On 14 July, the CME arrived at L1 with a shock observed by the *Wind* spacecraft at 17:38 UT, followed by the shock sheath and a two-day long magnetic cloud

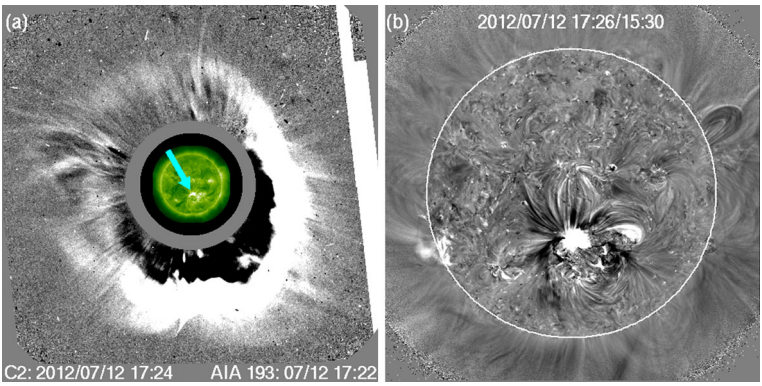

Figure 1 Images showing the solar source region on 12 July 2012. (**a**) SOHO/LASCO running-difference image showing the full-halo CME on 12 July, 17:24 UT. Superimposed within the occulting disk area is an *Solar Dynamics Observatory* (SDO)/AIA image at 193 Å at nearly the same time with the *arrow* pointing to the near-disk center flare and dimming in AR 11520. This image is from the SOHO/LASCO CME catalog, which is generated and maintained at the CDAW Data Center by NASA and The Catholic University of America in cooperation with the Naval Research Laboratory. (**b**) Enlarged AIA base-difference image of the source region.

(MC, see Figure 2). Strong southward-directed interplanetary magnetic field (IMF), with a peak flux of 16.7 nT in the MC produced a moderate geostorm with beautiful aurora over the Earth, extending to 15 July. The sheath persisted for $\sim$14 hours until the magnetic cloud and flux rope arrived at Earth at $\sim$07:00 UT on 15 July. Marubashi, Cho, and Ishibashi (2017) noted that the source region magnetic fields implied that the front of the flux rope should have had northward fields. That the fields were southward indicates the spacecraft passed through the back of the flux rope (see their Figure 2). The rope was an east–south–west type (right handed, RH), with the flux rope axis pointing southward. The total field had a peak of 28.4 nT, which steadily decreased as the rope passed the spacecraft. The velocity also gradually decreased, indicating an expanding flux rope, and, as expected, low density and temperature in the magnetic cloud. This ICME drove a moderate, long-lived geomagnetic storm with peak Dst $= -127$ nT on 15 July and with a duration of several days (Figure 2, top panel).

On 12 July 2012, SWPC issued its three-day forecast at 22:00 UT, after the flare, calling for geomagnetic active levels up to minor storm (G1, Kp $= 5$) level on 14 – 15 July. Indeed, Kp was ≥ 5 from 14 July into 16 July (Figure 3), so this forecast was mostly successful. However, since Kp reached 6 (G2), on 15 July, the storm was slightly underpredicted. This VarSITI campaign event is considered to be a textbook case in that we could identify the complete chain of a single well-observed Sun-to-Earth event from its solar source, through its heliospheric propagation to its geoeffects. The propagation kinematics, flux rope eruption, and magnetohydrodynamic (MHD) modeling for this event were well analyzed by WG 4 members and others (*e.g.* Gopalswamy *et al.*, 2013; Hess and Zhang, 2014; Shen *et al.*, 2014; Möstl *et al.*, 2014; Cheng *et al.*, 2014; Dudík *et al.*, 2014; Hu *et al.*, 2016; Marubashi, Cho, and Ishibashi, 2017).

Gopalswamy *et al.* (2013) argued that at least the shock arrival for this event was delayed because the CME was significantly deflected to the west–northwest by a large coronal hole (CH) on the eastern half of the solar disk. Whether the open magnetic field lines from large CHs can greatly influence the propagation of CMEs remains an active area of research.

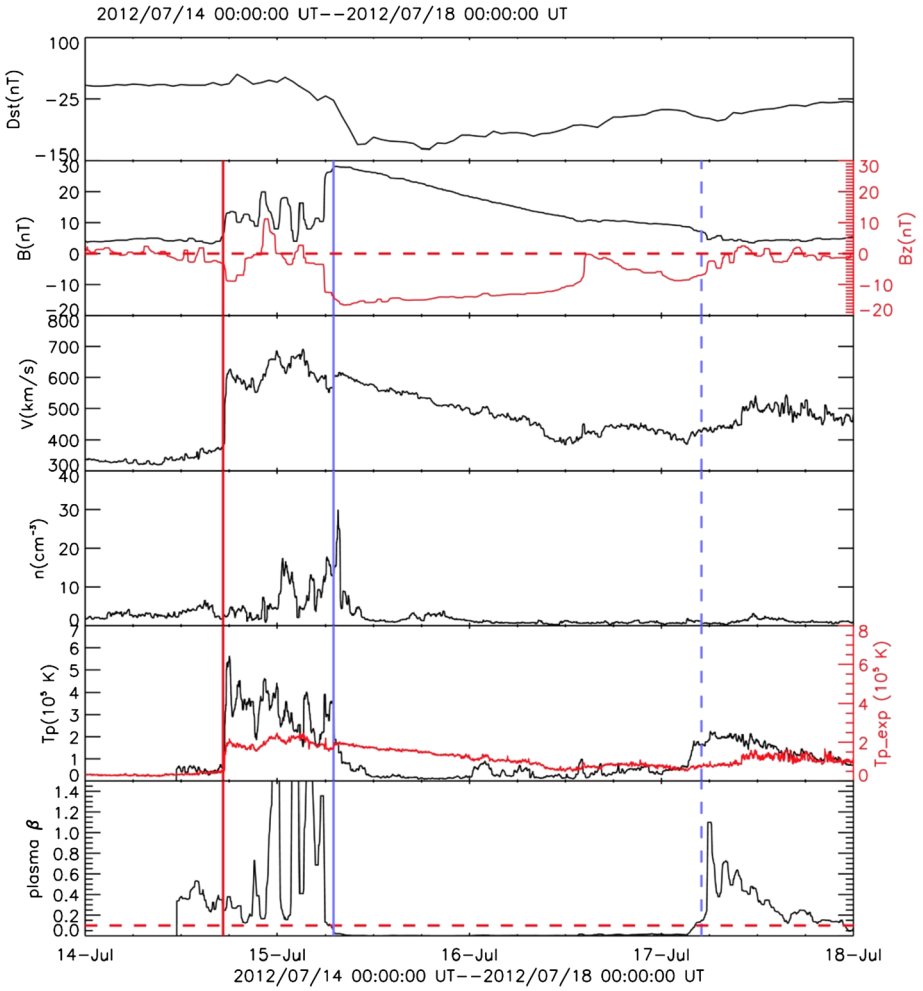

Figure 2 Solar wind measurements at ACE at L1 from 14 – 18 July 2012. The shock is denoted by the *vertical red line* and the ICME by the *solid* and *dashed blue lines*. The *plots* from *top* to *bottom* show the Dst index, the total magnetic field and its Z component (*red*), the velocity, the density, the proton temperature with the expected temperature derived from the velocity in *red*, and the plasma β. From Hess and Zhang (2014). Reproduced by permission of the AAS.

2.3. A Possible Textbook but Complex Case

The 21 – 24 June 2015 case was a compound *in situ* event resulting from a series of four shocks arriving over a three-day span, and one likely ICME at 1 AU on 23 – 24 June. The third shock and ICME were likely produced by a symmetric halo CME on 21 June. The southward field in multiple shock sheaths and the ICME drove a powerful multi-step geostorm reaching Kp = 8 (G4, see Figure 4a) and Dst = −204 nT (Figure 5) on 22 – 23 June. Although many researchers considered this a "superstorm", the usual definition of a superstorm requires a Dst ≤ −250 nT (*e.g.* Gonzalez *et al.*, 2002).

The 3-Day Forecast issued by NOAA/SWPC at 21 June 2015, 22:00 UT stated: "The geomagnetic field is expected to be at unsettled to severe storm levels on day one (22 Jun),

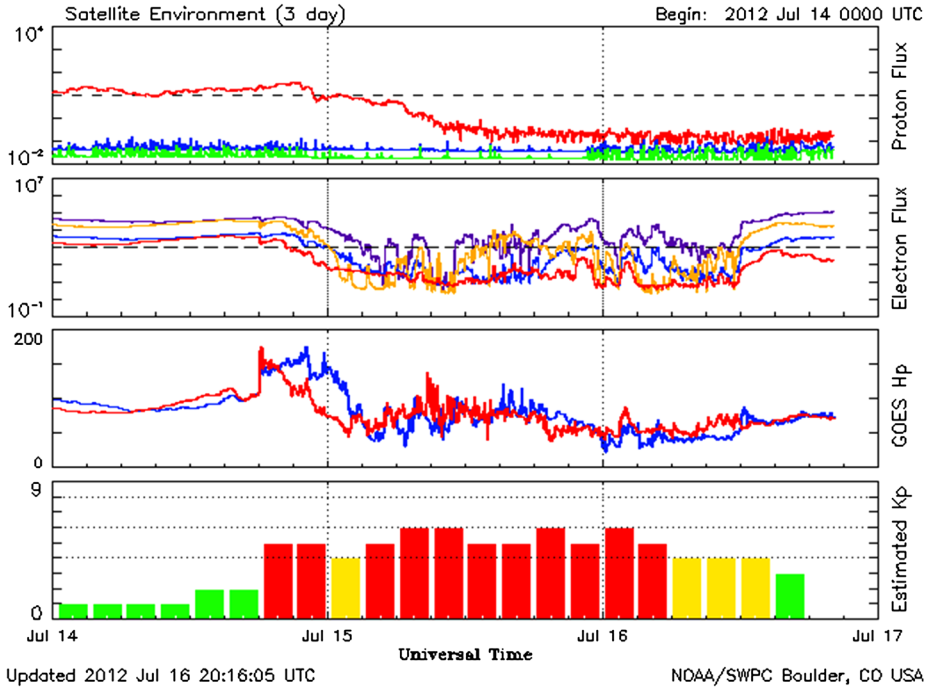

Figure 3 Three-day satellite environment plot from NOAA/SWPC showing the proton and electron fluxes, the GOES Hp in nT, and at the *bottom* the Kp index, showing the storm from 14 – 16 July.

unsettled to major storm levels on day two (23 Jun) and quiet to active levels on day three (24 Jun). Protons are expected to cross threshold on day one (22 Jun), are expected to cross threshold on day two (23 Jun) and are likely to cross threshold on day three (24 Jun)."

Independently of NOAA, coauthor Nitta tweeted on 21 June: "Almost circular halo CME (Earth-directed, expected arrival 23/24 June)... associated with M flare. Nice dimming." The images shown in Figure 4b were attached to this tweet, which also proved to be a good "forecast". This fast (1300 km s^{-1}) halo CME occurred on 21 June and was associated with an M2.6 flare at N12 E13 peaking at 01:42 UT.

This therefore was a successful forecast in that strong to severe storm (Kp = 7 – 8+) levels were reached on 22 – 23 June. The 21 June symmetrical halo CME was the main source (see below). The proton flux was also enhanced on all three days.

Thus, from an "official" forecast view, this was a textbook case, except that it was slightly inaccurate since it reached the severe storm level on 23 June rather than 22 June. However, there were four flares with filament eruptions and CMEs from AR 12371 on 18 – 22 June as it rotated toward the central meridian, which led to the multiple shocks, sheaths, and the ICME at L1 (Figure 5). These produced a compound event and storm, complicating our understanding of the Sun–Earth chain.

This VarSITI campaign period has been well studied by WG 4 and by many in the magnetospheric–ionospheric community. Figure 5, taken from Liu *et al.* (2015), shows *in situ* data from the *Wind* spacecraft at L1. The four shocks are denoted by the dashed vertical lines. Liu *et al.* identified the main ICME as lying within the gray band starting on 23 June at 02:00 UT, with S3 being its preceding shock. They also reconstructed two small flux ropes within the same ICME, both with high elevation angles and similar left-handed

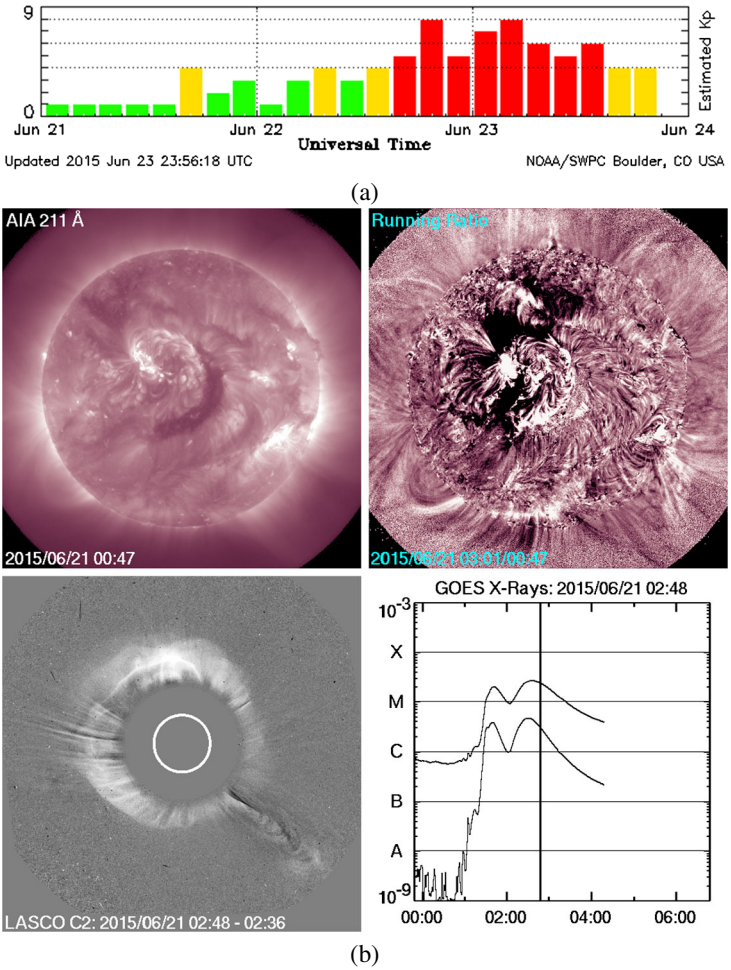

Figure 4 Data for the 21 – 24 June 2015 event period. (**a**) NOAA/SWPC plot of the Kp index for three days from 21 – 24 June. The *red bars* indicate the storm levels with Kp > 4. (**b**) Images showing the 21 June flare and dimming region in AIA 211 Å (*top panels*) and the symmetric halo CME and GOES X-ray plot (*bottom panels*). This fast (1300 km s^{-1}) halo CME was associated with the M2.6 flare at N12 E13, peaking at 01:42 UT. The *bottom images* are from the SOHO/LASCO CME catalog, which is generated and maintained at the CDAW Data Center by NASA and The Catholic University of America in cooperation with the Naval Research Laboratory.

(LH) orientations. There was some controversy, however, about this as Marubashi, Cho, and Ishibashi (2017) assumed that there was only a single magnetic cloud, on 23 June from 02:00 to 12:00 UT. They were able to fit two possible torus geometries to the flux rope, one RH and the other LH. However, they were not able to make a clear connection between a single solar source event and the *in situ* flux rope.

This series of CMEs was observed in the heliosphere as enhanced interplanetary scintillation (IPS) density structures from 19 – 26 June 2015 (Manoharan *et al.*, 2016). In particular, the halo CMEs leading to the severe storm were imaged as halo structures from 22 – 24 June (Figure 2 in Manoharan *et al.*, 2016). The solar wind speed reached $\sim$ 1000 km s^{-1}. From

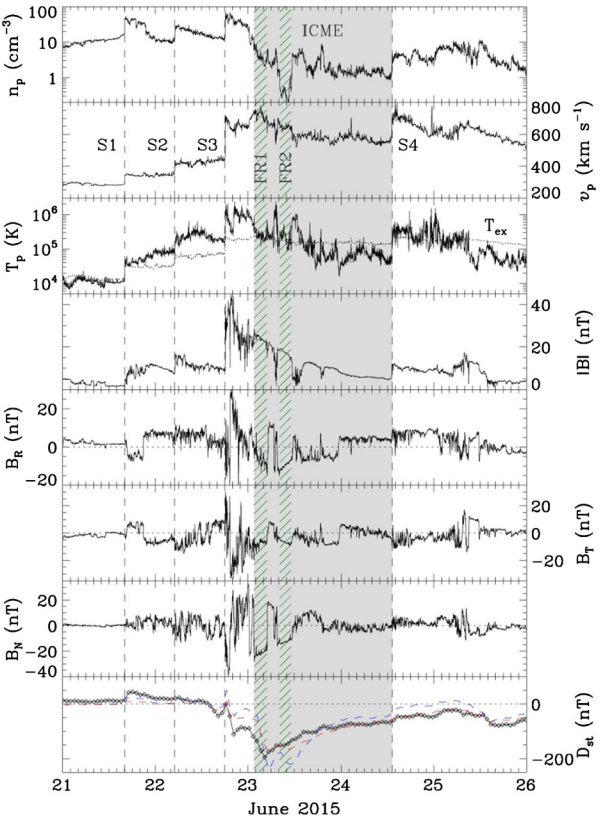

Figure 5 Solar wind measurements at *Wind* and associated Dst index for the 22 – 24 June 2015 event. The *shaded region* shows the overall ejecta interval, while the *hatched areas* indicate two small flux ropes identified within the ICME. Three shocks are observed ahead of the ejecta. The last shock (S4) was driven by the CME that occurred at the Sun on 22 June and was overtaking the ICME at 1 AU. From Liu *et al.* (2015). Reproduced by permission of the AAS.

the *in situ* data, Liu *et al.* (2015) concluded that this was a multi-step, or compound, storm driven by strong southward fields in two shock sheaths (S2 and S3), and especially, in the first flux rope of the ICME. This period also had high solar wind speed within and following the ICME, which probably helped to compress and enhance the fields.

As a VarSITI Campaign event, this case was very interesting from the geoactivity standpoint. From the *Advanced Composition Explorer* (ACE) spacecraft data on 22 – 23 June, Reiff *et al.* (2016) highlighted the high proton density and flow pressure behind the (third) shock and before the ICME. WG 4 member E. Kilpua (2015, private communication) first noted the likely effect this high pressure had on the ring current and, therefore, on the Dst. The strongest $-B_Z$ intervals and the minimum Dst in the event were preceded by northward IMF (Figure 5, seventh panel) and the high density in the shock sheath (top panel). Such conditions likely combined to produce a particularly dense plasma sheath in the magnetosphere and enhanced the ring current upon arrival of the strong $-B_Z$ field related to the first flux rope (seventh panel).

N. Lugaz (2015, private communication) noted that shock S3, combined with the high dynamic pressure and long-duration southward field, greatly compressed the magnetosphere (see Figure 8 of Lugaz *et al.*, 2016). Lugaz *et al.* (2016) considered this a case of a shock propagating inside the sheath of a preceding shock. The core of the ICME itself had very low density and the solar wind likely had a low Mach number, around S1. Finally, shock S4 was probably driven by a fast (~ 1000 km s^{-1}) CME associated with an M6.5 flare on 22 June from N13 W05 peaking at 18:36 UT. The ICME behind shock S4 also had high speed and

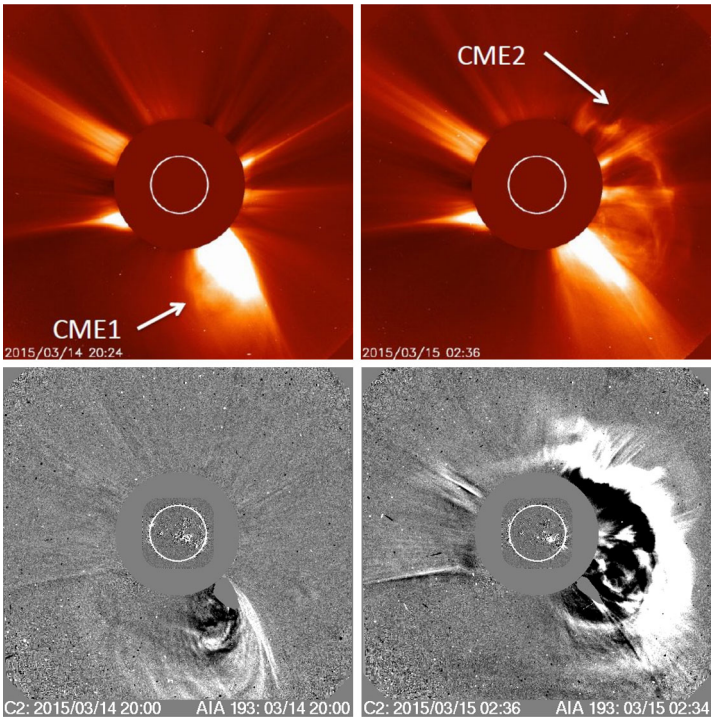

Figure 6 Two possible source CMEs launched on 14 and 15 March 2015. *Top*: direct SOHO/LASCO C2 images. The *left image* is 14 March at 20:24 UT and the *right image* is 15 March at 02:36 UT. *Bottom*: SOHO/LASCO C2 running-difference images. The *left image* is 14 March at 20:20 UT and the *right image* is 15 March at 02:36 UT. Superimposed within the occulting disk area are SDO/AIA running-difference images at 193 Å showing the bright source active region: the *left image* is 14 March at 20:20 UT and the *right image* is 15 March at 02:34 UT. The *top images* are courtesy of M. Temmer (2015, private communication). The *bottom images* are from the SOHO/LASCO CME catalog, which is generated and maintained at the CDAW Data Center by NASA and The Catholic University of America in cooperation with the Naval Research Laboratory.

was probably overtaking the preceding, slower ICME. This later ICME, on 24 – 25 June, was not geoeffective, however, probably because the magnetic field was not strongly southward (Figure 5, seventh panel).

2.4. A Problem Case: Storm Underpredicted but Now Understood

The first *severe* storm of Cycle 24 occurred on 17 – 18 March 2015, the so-called St. Patrick's Day storm. It has generated much interest; *e.g.*, as a VarSITI campaign event, a special Joint Geospace Environment Modeling-Coupling Energetics and Dynamics of Atmospheric Regions (GEM-CEDAR) campaign event, and a *Journal of Geophysical Research* special volume (*J. Geophys. Res.*, **121**, 2016). Given the relatively weak preceding solar activity and CMEs that were offset over the south and west solar limb, however, only a minor storm was forecast. Thus, this was a problem forecast (T. Berger, 2015, private communication).

A slow (350 km s^{-1}) CME occurred to the south–southwest late on 14 March likely associated with a small C2.6 flare, peaked at 11:55 UT, from AR 12297 at S21 W20 with a small filament eruption. Then on 15 March, $\sim$01:36 UT, a fast (1120 km s^{-1}), asymmetric

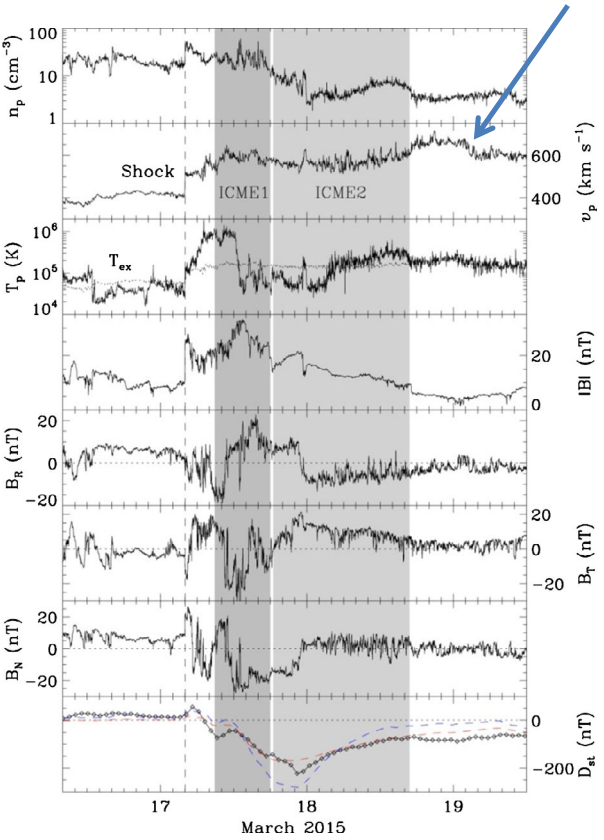

Figure 7 *In situ* observations of the solar wind from the *Wind* spacecraft at L1. Data are from 16 – 19 March 2015, with the *dashed vertical line* denoting the shock and shaded regions noting the two proposed ICMEs. The *arrow* points to the high-speed stream. Adapted from Liu *et al.* (2015).

halo CME associated with a C9.1 flare erupted from the same active region, but was brightest over the west limb (Figure 6).

The 3-Day forecast issued by NOAA/SWPC on 15 March 2015 at 12:30 UT stated: "Initial analysis of coronagraph imagery and subsequent WSA-Enlil model output suggests a glancing blow from the western flank of the CME very late on 17 Mar into 18 Mar. G1 geomagnetic storms are likely on day three (18 Mar) due to a combination of CME activity from 15 Mar as well as recurrent coronal hole high speed stream effects."

In situ observations at L1 showed that a strong shock struck the *Wind* spacecraft on 17 March at 04:01 UT, followed by an extended sheath, then an ICME and a MC from 17 March at 12:30 to 23:20 UT (Figure 7). Behind the cloud were a CIR and its high speed stream (arrow in Figure 7). The solar wind parameters were likely enhanced due to this fast stream. These regions included strong southward fields in the sheath and the MC, which drove a two-step, or compound, storm (see the two bottom panels of Figure 7) (*e.g.* Liu *et al.*, 2015; Kamide and Kusano, 2015; Kataoka *et al.*, 2015; Marubashi *et al.*, 2016). The sheath magnetic field produced the first storm dip and the field in the magnetic cloud(s) drove the second, longer dip. The minimum Dst was −223 nT, reached on 17 March at 23:00 UT, identified as a severe storm with a Kp = 8. So the NOAA forecast very much underpredicted this storm in terms of both its magnitude and early time of arrival.

The question then is, what happened? Our discussions revealed different interpretations about the entire chain from the source regions, any interactions or deflections affecting the

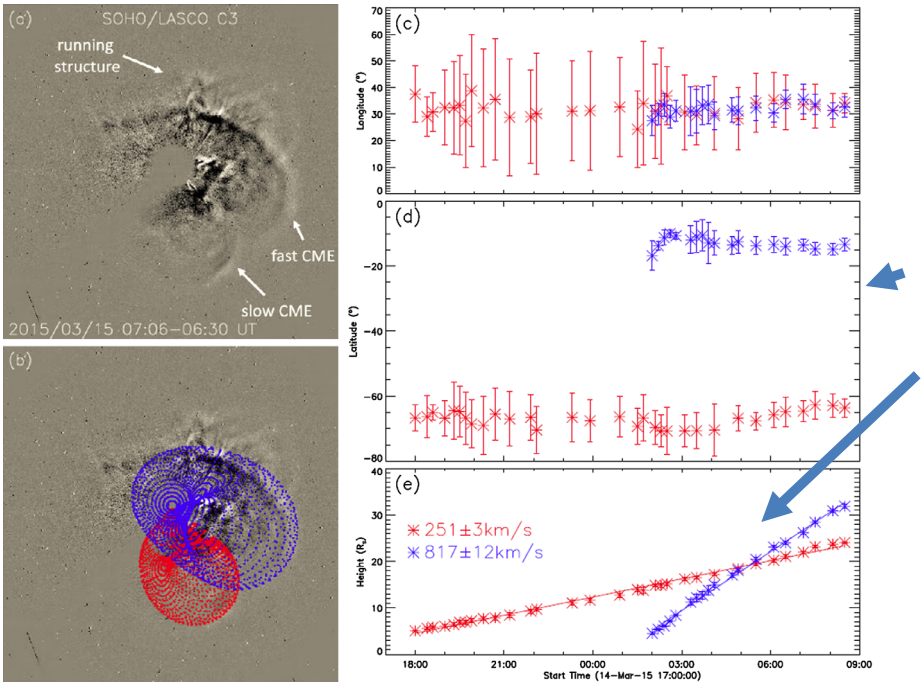

Figure 8 Evidence for a lack of interaction between the two CMEs on 14 – 15 March 2015. (**a**) SOHO/LASCO C3 difference images showing the 15 March fast CME and the preceding 14 March slow CME, and (**b**) the same with the GCS fits superimposed. The *right-hand panels* show the (**c**) longitudes, (**d**) latitudes, and (**e**) heights of the leading edges of the two CMEs obtained from the GCS fitting. The *lines* in panel **e** are the linear fits to the CME heights, assuming a reasonable uncertainty of ± 1 R_S. From Wang *et al.* (2016).

propagation, and the signatures at Earth. These differences are highlighted in two detailed articles by Liu *et al.* (2015) and Wang *et al.* (2016). Starting with the sources, the first CME involved the disruption of a preexisting streamer. Did this streamer lie on the frontside or backside of the Sun? Liu *et al.* (2015), along with P. Hess and M. Temmer (2015, private communication), concluded that it was frontside and associated with AR 12297 and that this and the later CME interacted, resulting in two ICMEs at L1 (as noted in Figure 8). Wang *et al.* (2016) agreed with N. Gopalswamy and S. Yashiro (2015, private communication) that this CME was a backside event because the preexisting white-light streamer was moving toward the South pole, suggesting that its location was on the backside. Thus, the preceding slow CME was unlikely to have interacted with the later fast CME. Using the graduated cylindrical shell (GCS) 3D reconstruction model (Thernisien, Howard, and Vourlidas, 2006) on the two events (Figure 8a – b), Wang *et al.* concluded that since they were widely separated in latitude by $\sim 50°$ (Figure 8d), and because there was no clear acceleration of the slow CME or deceleration of the fast CME, as might be expected if they physically interacted (Figure 8e), only the later fast CME was geoeffective.

This controversy is reflected in the interpretations of the *in situ* data. Liu *et al.* (2015) concluded that there were two separate ICMEs at L1. Using a Grad–Schafranov (G–S) fitting, these authors concluded that there were two flux ropes, both RH with opposite orientations. Both had low elevation angles, consistent with the polarity inversion line (PIL) and filament channel in the AR being nearly horizontal, as described by N. Gopalswamy and M. Temmer

(2015, private communication). Wang *et al.* (2016), Marubashi *et al.* (2016), Marubashi, Cho, and Ishibashi (2017), and Wu *et al.* (2016) independently assumed there was a single ICME and flux rope that could be fit from about 17 March at 12:00 to 18 March, 00:00 UT (Figure 7). Wang *et al.* fit the flux rope with their velocity-modified cylindrical flux rope model (Wang *et al.*, 2015) and with a G–S reconstruction. Both yielded RH flux ropes with similar orientations. Marubashi *et al.* (2016) derived several possible flux rope structures using toroidal and cylindrical models that fit the observed IMF variation of the single flux rope. Given the *in situ* fits combined with the expected orientation from the source PIL, they concluded that the flux rope was toroidal. The plane of the toroid was nearly parallel to the ecliptic and the spacecraft passed through the eastern flank of the structure. Finally, Wang *et al.* (2016), Marubashi, Cho, and Ishibashi (2017), and Wu *et al.* (2016) all mentioned the possibility of a second weaker flux rope with northward fields following the first on 18 March at about 01:00 UT.

Wang *et al.* (2016) also modeled the propagation speed and trajectory of the CME to Earth. According to Wang *et al.* (2015), the velocity components of the flux rope fit suggest that the CME was deflected eastward by $\sim 12°$, moving its path closer to the Sun-L1 line, and, therefore, enhancing its geoeffectiveness. Additional calculations were made using a background solar wind from a 3D MHD simulation for Carrington rotation 2161 (Shen *et al.*, 2011) and adjusting the CME speed with the Drag-Based Model (DBM; Vrsnak *et al.*, 2013). These results were consistent with the time of arrival and speed of the leading front of the CME. C. Möstl (2015, private communication) used the Ellipse Evolution (ElEvo) model (Möstl *et al.*, 2015) to predict that the axis of the CME would propagate 40° west of the Sun–Earth line. That a strong MC hit L1 and Earth suggests that there was significant deflection of the CME toward Earth, in agreement with Wang *et al.*'s conclusion. This deflection was likely influenced by the CIR and high-speed stream.

From NOAA's viewpoint, running the Wang–Sheeley–Arge Enlil (WSA-Enlil) model with the source CME $\sim 20°$ farther to the east would have produced a forecast of a stronger storm and a more accurate arrival time. This illustrates the problems forecasters have in selecting not only the "correct" event and its launch location at the Sun, but also its final propagation trajectory (T. Berger, 2015, private communication). Wu *et al.* (2015) also simulated the event using the global 3D time-dependent MHD model (H3DMHD) to study this CME propagation to Earth. The model was driven by solar wind data at the inner boundary, 40 R_S, of the computation domain. The model used time-varying 3D solar wind proton velocity and density values reconstructed from IPS data and the magnetic field inner boundary as provided by a Current-Sheet Source Surface (CSSS) closed-loop propagation model (*e.g.* Jackson *et al.*, 2015). This simulation matched the peak magnitude of the shock and its arrival time at *Wind* well.

2.5. A Problem Case: Storm Overpredicted but Now Understood

On 10 September 2014, an X1.6 flare erupted in AR 12158, peaking at 17:45 UT at N15 E00. As shown in Figure 9a, this event was centered on the disk and had a large dimming region and a rapidly expanding coronal wave (top right). The lower left image shows the fast ($1400\ km^{-1}$) symmetric halo CME (onset at 18:12 UT) associated with the flare. This event seemed like a textbook example: a major storm was predicted, and indeed, a strong shock hit Earth on 12 September, followed by an MC extending into 13 September. However, the storm was relatively small ($Dst = -73$ nT) and uneventful (Figure 9b). What happened?

The 3-Day forecast issued by NOAA/SWPC on 10 September 2014 at 22:00 UT, after the flare, stated: "The geomagnetic field is expected to be at quiet levels on day one (11 Sep),

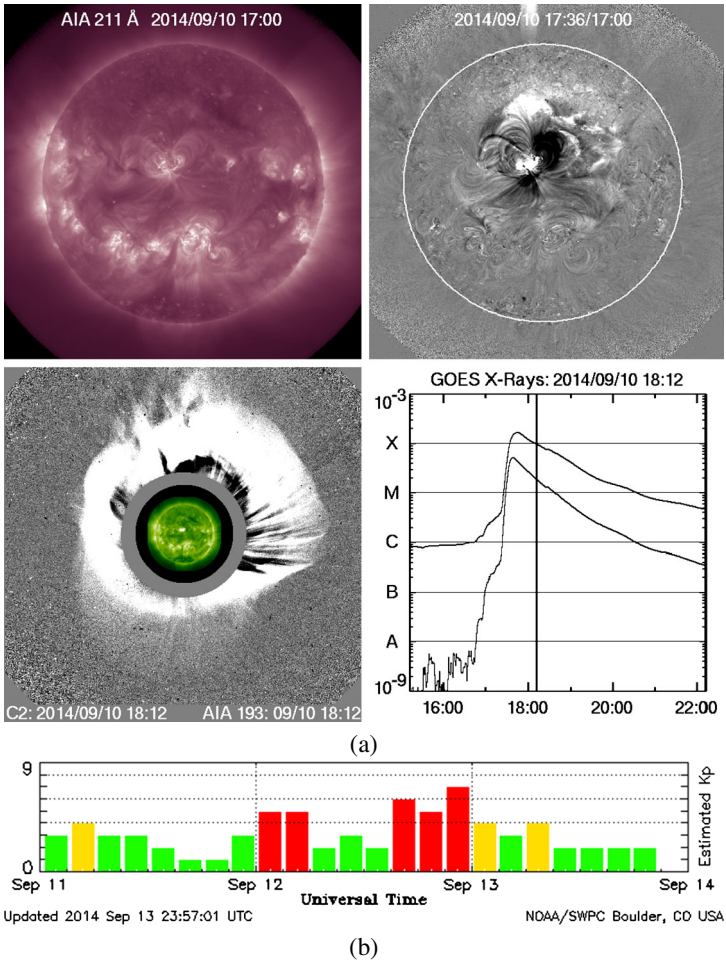

Figure 9 Data for the 10 – 14 September 2014 event period. (**a**) The *top images* are of the northern source region on 10 September 2014 in both SDO/AIA 211 Å direct (*left*) and base-difference images (*right*). The *bottom images* are (on the *left*) SOHO/LASCO C2 difference image of the symmetrical halo CME with an AIA 193 Å image superimposed within the occulting disk area, and (on the *right*) the GOES plot of the X-ray event. These images are from the SOHO/LASCO CME catalog, which is generated and maintained at the CDAW Data Center by NASA and The Catholic University of America in cooperation with the Naval Research Laboratory. (**b**) NOAA/SWPC plot of the three-hour estimated Kp index from 11 – 14 September 2014. *Red bars* show Kp levels > 4.

quiet to major storm levels [strong = G3] on day two (12 Sep) and quiet to minor storm levels on day three (13 Sep).” The next day forecast was: “The geomagnetic field is expected to be at unsettled to major storm levels on day one (12 Sep), active to severe storm levels on day two (13 Sep) and unsettled to minor storm levels on day three (14 Sep).” Thus, the forecasted level on 13 September was raised to severe, or G4 (Kp = 8), level.

The WAS-Enlil model runs at SWPC and others at NASA/GSFC Space Weather Research Center (https://kauai.ccmc.gsfc.nasa.gov/CMEscoreboard/PreviousPredictions/2014;jsessionid=92018E2AC18F90D2C18011E523670437) showed a direct hit at Earth, and the average shock-time arrival was accurate to within a few hours (shock arrival at ACE was on

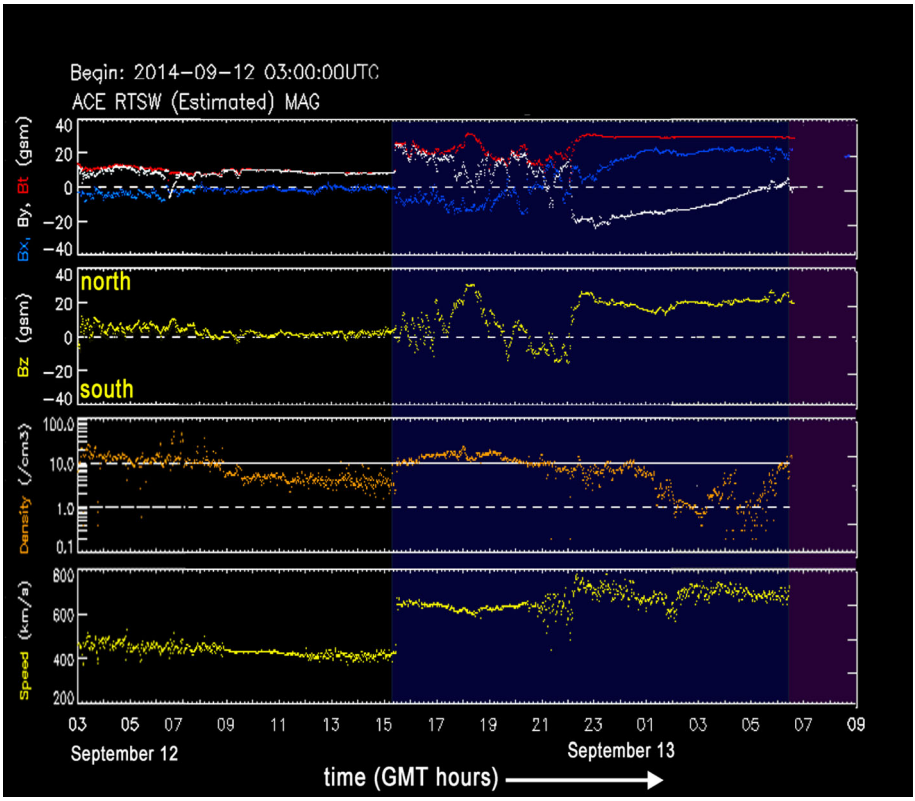

Figure 10 ACE real-time solar wind parameters as displayed by NOAA/SWPC from 12 September 2014 at 03:00 UT to 13 September 2014 at 09:00 UT. A strong shock struck on 12 September at 15:26 UT followed by a prolonged sheath region then a fast ICME with a long-lived MC. The magnetic fields in the sheath and the MC were almost entirely northward ($+B_Z$), however, thus shutting off the brief, minor storm. Adapted from the NOAA/SWPC website by T. Skov (2015, private communication).

12 September at $\sim$ 15:26 UT). However, as Figure 9b shows, the actual storm was brief and reached a Kp of 7 (G3) for only one three-hour interval, but was otherwise minor (G1 level).

Figure 10 shows the ACE real-time solar wind parameters as displayed by NOAA/SWPC. Following the shock, there was strong total magnetic field ($B \sim 35$ nT, red line in the top panel of Figure 10) in the sheath and in the long-duration MC, extending into 13 September. However, the fields in most of the sheath and MC were almost entirely *northward* ($+B_Z$, yellow line in second panel). The storminess was driven by the brief period of a southward field in front of the MC.

Since the source AR was isolated and the flare and its arcade outlined an apparently well-organized PIL, several WG 4 members, particularly C. Möstl and V. Bothmer (2015, private communication), made predictions of the orientation and geoeffectiveness of the expected flux rope. Unfortunately, there was no consensus except that the flux rope should be LH. Marubashi, Cho, and Ishibashi (2017) successfully fit the MC as a LH toroidal flux rope, but its orientation was not consistent with the X1.6 flare and CME (Figure 9a) source parameters. His colleagues later discovered that there was a second later eruption in the AR along a western PIL, which agreed with the flux rope fit orientation (Figure 11). From the SDO/AIA and *Helioseismic and Magnetic Imager* (HMI) images, the PIL orientation of the flare re-

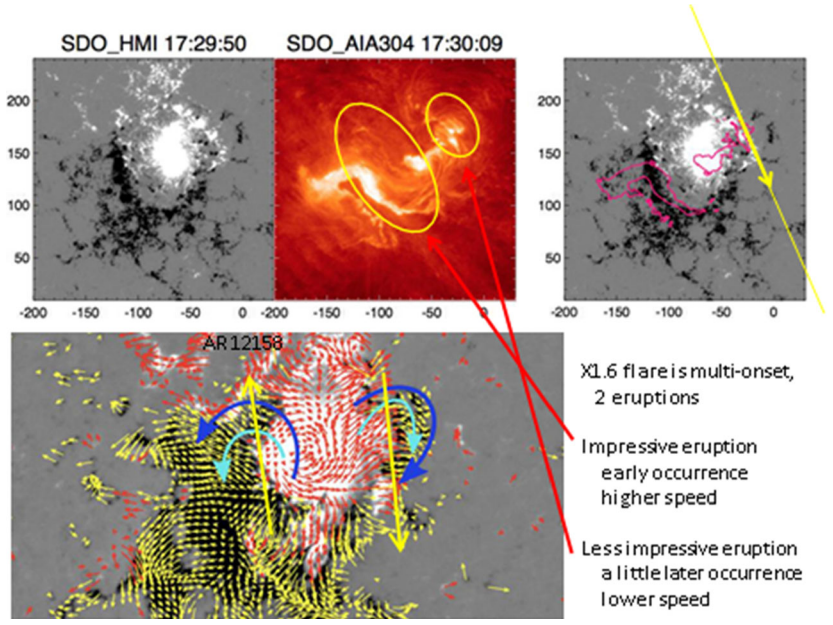

Figure 11 Images supporting that the 10 September 2014 X1.6 flare was actually a multi-onset event, or two separate eruptions: one at N15 E07 and the other at N17 E03, both in AR 12158. *Top*: Images of the photospheric field in SDO/HMI and the flare ribbons in SDO/AIA 304 Å. *Bottom*: An HMI vector field map showing the opposite directions of the eastern and western PILs (*yellow arrows*) involved in the two eruptions. The curving *blue arrows* indicate the direction of the pre-existing close magnetic loops. Marubashi, Cho, and Ishibashi (2017) claim that the later western PIL was associated with the flux rope fitted at 1 AU. Figure courtesy of K. Marubashi (2017, private communication).

gion in AR 12158 was estimated to be 245° (K. Marubashi, 2015, private communication). The flux rope fit result yielded an orientation of 247°, thus, close to the corresponding PIL orientation. The main body of the flux rope lay above the ecliptic plane such that the spacecraft, and Earth, crossed near its southern edge where the IMF was northward throughout the passage. In summary, this storm was overpredicted, but we think we now understand why. However, this process illustrates how difficult it can be to properly interpret solar images *in near-real time* so that we understand the potential geoeffectiveness of an event.

2.6. A Problem Case: Storm Underpredicted and Source Unclear, with Multiple and Weak Signatures, but Now Understood

The 4 – 9 October 2012 case was a problem campaign event, which was initially chosen as the best example of this type, but we think we now understand it. The source was likely a single CME, and a resulting ICME with an MC, that drove a G2 (Kp = 6+) storm. This CME appeared as a partial halo (Figure 12) that was first observed in SOHO/LASCO C2 on 5 October at 02:48 UT and in STEREO-A coronagraph COR2 at 02:24 UT with an estimated C2 plane-of-sky speed of 612 km s^{-1}. NOAA/SWPC identified this CME, and their WSA-Enlil model indicated it might be geoeffective late on October 8. There were only weak and multiple solar surface signatures, however, making it difficult to identify the source region location and the timing. The 3-Day Forecast issued by NOAA/SWPC on 5 October 2014 at 22:00 UT, after CME onset, stated: “Late on day 3 (08 October), todays CME is

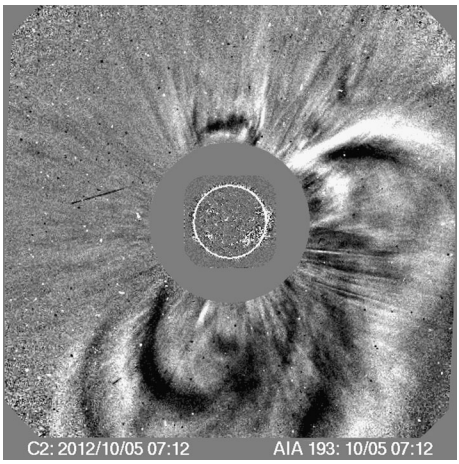

Figure 12 SOHO/LASCO running-difference image showing the full-halo CME on 5 October 2012 at 07:12 UT. Superimposed within the occulting disk area is an SDO/AIA 193 Å running-difference image at the same time. The bright area in the southwest is associated with AR 11584 and a post-eruption arcade (PEA) and slow dimming that Nitta and Mulligan (2017) identified as the source region. These images are from the SOHO/LASCO CME catalog, which is generated and maintained at the CDAW Data Center by NASA and The Catholic University of America in cooperation with the Naval Research Laboratory.

expected to become geoeffective causing unsettled to active conditions with a chance for minor storm periods." The next day forecast was: "An increase to unsettled to active levels with a chance for minor storm periods is expected on days two and three (08 – 09 October) as the 05 October CME is forecasted to arrive." Thus, the timing of a storm was predicted, but only to the minor (G1) level.

The solar source region of this CME and associated ICME has been investigated for some time by WG 4. M. Temmer (2012, private communication) pointed out that this was not a "stealth" CME (*e.g.* Howard and Harrison, 2013) in the sense of having no solar surface signatures at all, but instead a "silent" CME in that it was difficult for space weather forecasters to identify. P. Hess (2012, private communication) identified a very small disturbance at S22 W38 just before 00:00 UT on 5 October, clearest in AIA 304 Å images. C. Möstl (2012, private communication) noted an eruption on 4 October at 15:00 UT in AIA movies, two other minor eruptions on 4 October at 07:00 UT, slightly west of disk center, and at 09:30 UT, in the southeast quadrant. During a discussion at the China ISEST Workshop on 19 April 2014, the following points were made:

- From the GCS model based on STEREO-A and STEREO-B COR and SOHO/LASCO coronagraph data, the heliolongitude was W11, and the heliolatitude was S20.
- Around this position, there was a minor activity on 4 October at 14:00 – 15:00 UT seen in SDO/AIA 193 Å images. The activity appeared as a weak dimming followed by a diffuse brightening.
- In *Extreme Ultraviolet Imager* A (EUVI-A) 195 Å images after 4 October, 22:00 UT, there was a very faint eruption above the southeast limb. This beyond-limb faint eruption is consistent with the heliospheric position of S20 W11.
- The CME continued to accelerate to about 10 R_S with a peak speed of 800 $km\,s^{-1}$ on 5 October at 06:00 UT.

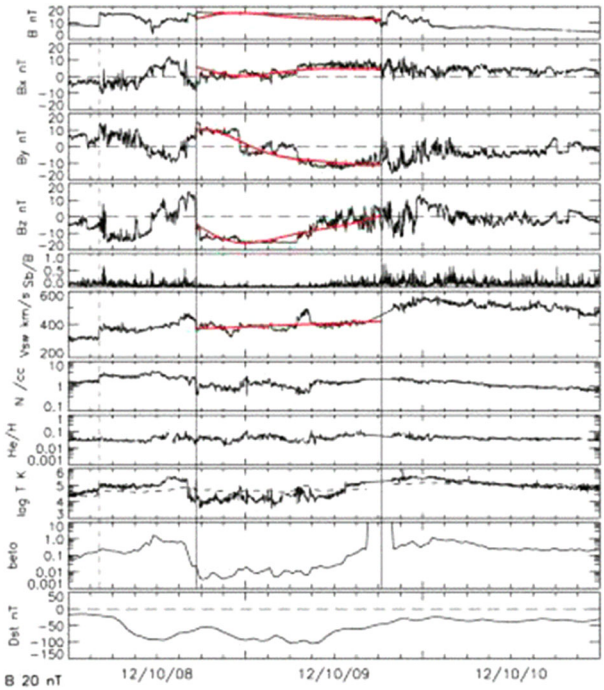

Figure 13 Solar wind data from *Wind* and the Dst variation for three days, 8 – 10 October 2012. From *top* to *bottom* are plotted the IMF intensity (B), X-, Y-, and Z-components in GSE coordinates (B_X, B_Y, and B_Z), the degree of field fluctuations defined by the standard deviation divided by the averaged intensity obtained from data with higher time resolution (Sb/B), solar wind speed (Vsw), proton number density (N), number density ratio of He++ to H+ (He/H), proton temperature, plasma β, and the Dst index. The *vertical dashed line* indicates the shock arrival time (on 8 October at 04:12 UT) and the *two vertical lines* indicate the flux rope (from 8 October at 17:20 UT to 9 October at 18:30 UT). The *red curves* show the model values obtained from the fitting with a toroidal flux rope model. Adapted from Marubashi, Cho, and Ishibashi (2017); courtesy of K. Marubashi (2017, private communication).

- If the eruption started on 4 October at 14:00 UT, it took a long time (10 hours) to reach the COR1 field of view. This suggests that the eruption had a long-lasting, low-speed, low-acceleration phase.

Nitta and Mulligan (2017) discussed this event in detail, essentially confirming the above interpretation relating the CME to the southwest region. They confirmed this with observations of dimmings in AIA 211 Å images and corresponding over-the-limb EUVI images in 284 Å images. These dimmings and a faint post-eruption arcade (PEA) were the low-coronal signatures of the CME. These signatures might also have been associated with a B7.6 flare in AR 11584.

Figure 13 from Marubashi, Cho, and Ishibashi (2017) shows the solar wind data from *Wind* and the Dst variation (eleventh panel) for 8 – 10 October 2012. The vertical dashed line indicates the shock arrival time and the two vertical lines indicate the MC observed from 8 October at 17:20 UT to 9 October at 18:30 UT. The red curves in this interval show the model values for their fit with a RH toroidal flux rope model. This was a two-step storm, caused by the southward field in the sheath and MC regions ($-B_Z$, fourth panel). The authors determined that the PIL orientation in AR 11584 was about 330°, with the magnetic field polarity positive (negative) on the south (north) side. The overall expansion of this CME

from this site is consistent with the PIL orientation. The flux rope geometry suggests that the flux rope propagated eastward from its solar origin, with the flux rope orientation estimated as 323°, very close to the PIL orientation. The magnetic field around the apex of the flux rope was northward, but the field at the first spacecraft contact with the flux rope was southward and the southward fields were long lived.

2.7. A Problem Case: Still Not Understood

This 27 May – 1 June 2013 case was a problem campaign event that we still do not understand. During this entire period, the NOAA/SWPC forecasts did not predict any geoactivity above minor storm level. On 1 June, however, there was a brief, strong storm (G3) that reached Kp = 7 and Dst = −119.

The clearest solar disk features showing activity occurred as much as five days before, on 27 May. Since the on-disk features were faint and subtle, it is obvious why no significant geoactivity was forecast, making this a stealth CME (see Nitta and Mulligan, 2017).

The *in situ* solar wind data (Figure 14) revealed a classic CIR at a sector boundary. I. Richardson (2013, private communication) noted possible forward (31 May at ∼ 17:30 UT) and reverse (2 June at ∼ 02 UT) shocks, and evidence of a stream interface (*e.g.* the increase in speed and temperature, and decrease in density on 1 June at ∼ 08:00 UT) within the CIR, preceded by the sector boundary. The slow-to-fast stream speed difference was quite large ∼ 300 – 800 km s^{-1}, also indicative of a well-formed CIR. The storm was mostly driven by the brief strong southward IMF "cutout" ($-B_Z$, ninth panel) from 00:10 – 06:40 UT on 1 June. Gopalswamy, Tsurutani, and Yan (2015) and Richardson and V. Bothmer (2013, private communication) agreed that the CIR with high-speed stream (HSS) alone was the cause of the storm. Gopalswamy, Tsurutani, and Yan (2015) noted that *in situ* observations showed that the CIR had a large magnetic field (∼ 25 nT) and the $-B_Z$ field, responsible for the storm, was also large (∼ − 20 nT).

However, there are several problems with this CIR–storm interpretation. First, a peak Dst > −110 nT is at the outer limits of what CIRs by themselves can produce (see, *e.g.* Richardson *et al.*, 2006). Compressed out-of-ecliptic fields are expected for a CIR or HSS, but the depth and duration of the south IMF notch in this event is unusual for a CIR. There was also evidence of an ICME in the flow, including the leading shock itself, and following the sector boundary and shock sheath, lower density (sixth panel) and plasma β (not shown). There was also evidence of rotations in the IMF, which was enhanced for more than one day.

The source of the CIR was a large, low-latitude CH that reached central meridian on May 29 – 30. The solar wind flow of its HSS reached ∼ 750 km s^{-1} on 2 June. There were several CME candidates, albeit weak, especially on 27 May, which could have been compressed by the HSS to cause the intense $-B_Z$ and the storm. In particular, A. Vourlidas (2013, private communication) noted that there were two north polar CMEs in LASCO images late on 26 May to early 27 May, one of the streamer-blowout type, and each having considerable extents toward the ecliptic. One had a very faint extension crossing the equator, indicating a partial-halo CME. The STEREO COR2 movies suggest that either or both of these CMEs could have been Earth-directed. In addition, there was some evidence in STEREO-A *Heliospheric Imager* 1 (HI1) movies of multiple fronts encountering Earth between 30 May and 1 June.

One reason for the lack of consensus is that the CME would have passed mostly north of the ecliptic, as evidenced by the COR and HI1 movies. However, M. Temmer (2013, private communication) noted a faint filament eruption from the northern extended PIL on 27 May at ∼ 09:30 UT. We consider the source location of the ICME to be centered at N10 E30, to

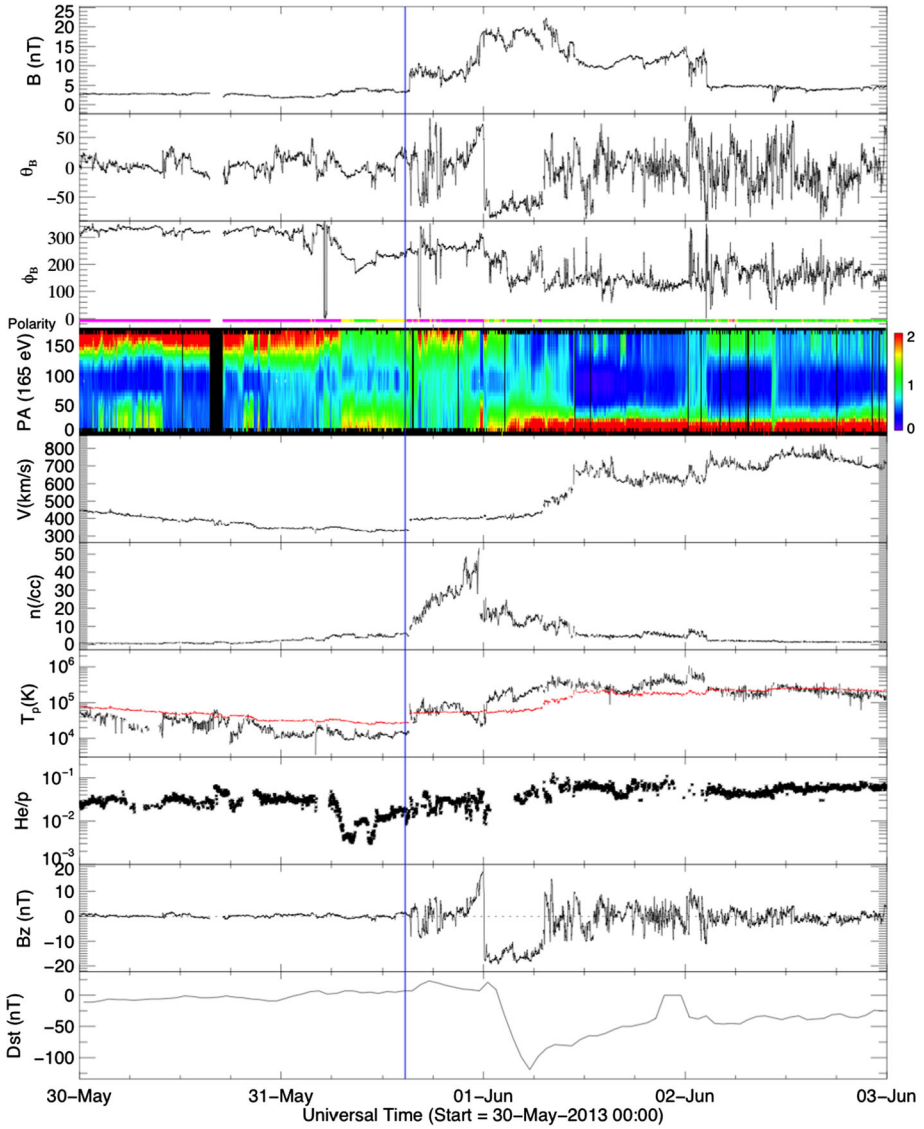

Figure 14 Solar wind data from *Wind* and the Dst variation from 30 May – 3 June 2013. From *top* to *bottom* are plotted the IMF intensity (B), the ecliptic latitude and azimuthal components, the position angles of 165 eV electrons, the solar wind speed, the proton number density, the proton temperature, the number density ratio of He/H, the IMF B_Z component, and the Dst index. The *vertical line* indicates the shock arrival time.

the north and west of the CH that was the source of the HSS. This region exhibited long-lasting coronal dimming in several AIA passbands on 27 May (Nitta and Mulligan, 2017). Thus, in general there was evidence of eruptive activity during 27 May associated with a long filament channel and arcade extending from the northeast solar limb to the central meridian. It is possible that the fast stream from the CH to the east of central meridian interacted with the 27 May post-CME flow, yielding the signatures at L1. This flow likely came from the

area just north of AR 11755, providing an organized ICME structure that was compressed in the CIR and HSS.

Finally, Marubashi, Cho, and Ishibashi (2017) examined the magnetic field variation during the *in situ* interval of a southward field on 1 June from 01:00 to 06:40 UT, to determine whether it might be interpreted as a flux rope structure. The *in situ* data could be fit with a torus model, suggesting that a small flux rope encountered the spacecraft. Examination of the IMF polarity sign indicates that the Earth was in the "toward" sector in the initial slow wind region and in the "away" sector in the high-speed stream (Figure 14, fourth panel). The "away" sector began at the rear boundary of the flux rope, and the Y-component of the solar wind velocity changed there from negative (westward) to positive (eastward). Thus, the authors concluded that the flux rope was inserted into the slow stream region and overtaken by the high-speed stream.

3. Summary

We summarize the results from our studies of each of these six cases to highlight the forecasting problems involved in each of them. Likely source CMEs were identified in all six cases, but the related solar surface activity ranged from uncertain or weak to X-class flares, and the CMEs had speeds ranging from slow to fast. The geoeffects ranged from none to severe as in the two Sun–Earth events in 2015. These six cases were chosen to illustrate some key problems in understanding the chain from cause to geoeffects. Five of the six events are VarSITI-wide campaign events and are, therefore, important to the other VarSITI groups. These problems, relative to how successful the forecast was, are noted in the last column of Table 1.

The 12 – 14 July 2012 case was considered a classic textbook event, in that we observed the complete chain of a well-observed Sun-to-Earth event, from its solar source through heliospheric propagation to its geoeffects. The propagation kinematics, flux rope eruption, and MHD modeling for this event were well studied by WG 4 members and others. The NOAA forecast was mostly successful for this event, but since the storm was only of moderate level, it was slightly underpredicted.

The 21 – 24 June 2015 case was also possibly a textbook event, but it was a *compound*, interesting event. The NOAA forecast of a severe storm was accurate, but that level was reached a day later than predicted. This severe level was reached because there were multiple shocks and sheaths, strong southward MC fields, and a high-speed solar wind that acted to compress and enhance the wind structures.

The 15 – 18 March 2015 case was initially a problem event, but we now understand why. This first severe storm of Solar Cycle 24 was underpredicted. Two flares and CMEs occurred at the Sun, but they were offset with regard to the Sun–Earth line. The CMEs may or may not have *interacted* near the Sun. Two detailed articles have argued either side of that argument. It is likely that during transport to Earth, there was *interaction* with a CIR and *deflection* toward Earth.

Although we did not discuss it, another of our study events, 7 – 9 January 2014, was considered a problem event at the time, but is now understood. It was a problem because a storm was predicted, but did not happen. Unlike the March 2015 case, in which the CME was deflected *toward* Earth, in this case the source flare and EUV wave were Sun-centered, but the *CME was offset* to the southwest, possibly *deflected* by a CH and/or *channeled* by strong AR magnetic fields, and thus it missed Earth.

The 10 – 12 September 2014 case was initially a problem event, but we now understand why. A major storm was predicted, and a strong shock and long-duration MC hit Earth. However, the storm was minor because the sheath and MC magnetic fields were *northward* ($+B_Z$), so the storm was overpredicted. WG 4 members tried to use PIL data to predict the expected flux rope orientation at 1 AU, but no consensus was reached.

The 4 – 9 October 2012 case was initially a problem event, but we now understand why. The source CME and resulting ICME that drove a small geostorm were forecast, but the storm was slightly underpredicted. There were *weak and multiple surface signatures* and the CME was initially very slow, however, leading to uncertainties in the arrival time.

Finally, the 27 May – 1 June 2013 case was a problem event that we still do not fully understand. During this entire period NOAA/SWPC did not forecast any geoactivity above the minor storm level. On 1 June, however, there was a brief but strong storm. A possible source was a slow CME on 27 May, but the associated *surface features were unclear*. There was also likely influence from a large CH. This led to interaction with a CIR and HSS at Earth with a likely embedded ICME. The ultimate *cause of the strong storm remains unclear*.

4. Conclusions

The goal of ISEST and WG 4 is to integrate observations, theory, and simulations to understand the chain of cause-effect dynamics from the Sun to Earth for a few carefully selected events. We wish to develop and/or improve the prediction capability for the arrival of these transients and their potential impacts at Earth.

WG 4 also examines more controversial events, such as stealth or "silent" CMEs and problem ICMEs, to enhance our understanding. An emphasis of WG 4 is on why forecasts fail and how we can improve our predictions. This includes analyzing the complications in linking CMEs to ICMEs, usually observed only *in situ*. After examination, we were left with results in three categories: (1) Textbook cases in which the complete chain of a well-observed event from a solar source is understood through its heliospheric propagation to its geoeffects. (2) Initially not textbook but problem events for which something is missing in the chain of a well-observed event, but in retrospect, we understand why. These cases usually involve predictions that failed because they were not geoeffective or were otherwise not accurate. (3) Finally, problem cases in which the chain is not complete and which we still do not understand.

Our July 2012 and June 2015 cases were considered textbook cases, but the forecasts were not fully accurate. The June 2015 case involved a compound event that likely pushed the level to a severe storm. The next three cases, March 2015, September 2014, and October 2012, were all considered problem events that we now understand. In March 2015, two CMEs possibly interacted near the Sun and were deflected by a CIR. In September 2014, the storm was overpredicted because the shock sheath and MC fields were almost entirely northward ($+B_Z$). For October 2012, a CME was identified, but the surface signatures were multiple and weak, leading to uncertainties in the arrival time. Finally, the last case in May–June 2013 was a problem event that we still do not fully understand. No storm was forecast, but a brief, strong storm occurred. The surface activities associated with a slow CME were unclear, as was the cause of the southward field ($-B_Z$) at 1 AU.

As in two of our cases, we note that about 20% of important geostorms have identified ICMEs but no compelling solar signatures. Moreover, about 10% of storms are due the compression of fields and plasma by CIRs and their HSSs (*e.g.* Zhang *et al.*, 2007). CIRs

played a role in two of our cases. The shock sheath region can also be very important for driving storms, as was the case in at least two of our events. A problem is that the sheath fields consist of swept-up coronal and heliospheric material, which makes them hard to predict in advance.

Acknowledgements We acknowledge the ISEST project, one of the four projects of the VarSITI program. VarSITI is sponsored and supported by SCOSTEP for the period a five-year period, 2014 – 2018. VarSITI is led by N. Gopalswamy, the President of SCOSTEP. We thank Jie Zhang for his leadership of ISEST and for organizing the ISEST workshops. We thank Jie Zhang and Phillip Hess for developing and hosting the ISEST event catalogs, data, and other information, which Working Group 4 has used extensively (see: http://solar.gmu.edu/heliophysics/index.php/Main_Page). We are grateful to these WG 4 members who contributed to the data analysis and results of the events that are presented here: Nat Gopalswamy, Phillip Hess, Emilia Kilpua, Bernie Jackson, Ying Liu, Noe Lugaz, Katsuhide Marubashi, Christian Möstl, Ian Richardson, Brigitte Schmieder, Kazuo Shiokawa, Manuela Temmer, Angelos Vourlidas, Yuming Wang, C-C Wu, and Jie Zhang. The SOHO/LASCO CME catalog is generated and maintained at the CDAW Data Center by NASA and The Catholic University of America in cooperation with the Naval Research Laboratory. SOHO is a project of international cooperation between ESA and NASA.

Disclosure of Potential Conflicts of Interest The authors declare that they have no conflicts of interest.

References

Baker, D.N., Li, X., Pulkkinen, A., Ngwira, C.M., Mays, L.L., Galvin, A.B., Simunac, K.D.C.: 2013, A major solar eruptive event in July 2012: defining extreme space weather scenarios. *Space Weather* **11**, 585. DOI.

Cheng, X., Ding, M.D., Zhang, J., Sun, X.D., Guo, Y., Wang, Y.M., Kliem, B., Deng, Y.Y.: 2014, Formation of a double-decker magnetic flux rope in the sigmoidal solar active region 11520. *Astrophys. J.* **789**, 93. DOI.

Dudík, J., Janvier, M., Aulanier, G., Del Zanna, G., Karlický, M., Mason, H.E., Schmieder, B.: 2014, Slipping magnetic reconnection during an X-class solar flare observed by SDO/AIA. *Astrophys. J.* **784**, 144. DOI.

Dumbović, M., Devos, A., Vršnak, B., Sudar, D., Rodriguez, L., Ruždjak, D., Leer, K., Vennerstrøm, S., Veronig, A.: 2015, Geoeffectiveness of coronal mass ejections in the SOHO Era. *Solar Phys.* **290**, 579. DOI.

Gonzalez, W.D., Tsurutani, B.T., Lepping, R.P., Schwenn, R.: 2002, Interplanetary phenomena associated with very intense geomagnetic storms. *J. Atmos. Solar-Terr. Phys.* **64**, 173. DOI.

Gopalswamy, N., Mäkelä, P., Xie, H., Yashiro, S.: 2013, Testing the empirical shock arrival model using quadrature observations. *Space Weather* **11**, 66. DOI.

Gopalswamy, N., Tsurutani, B., Yan, Y.: 2015, Short-term variability of the Sun–Earth system: an overview of progress made during the CAWSES-II period. *Prog. Earth Planet. Sci.* **2**, 13. DOI.

Hess, P., Zhang, J.: 2014, Stereoscopic study of the kinematic evolution of a coronal mass ejection and its driven shock from the Sun to the Earth and the prediction of their arrival times. *Astrophys. J.* **792**, 49. DOI.

Howard, T.A., Harrison, R.A.: 2013, Stealth coronal mass ejections: a perspective. *Solar Phys.* **285**, 269. DOI.

Hu, H., Liu, Y.D., Wang, R., Möstl, C., Yang, Z.: 2016, Sun-to-Earth characteristics of the 2012 July 12 coronal mass ejection and associated geo-effectiveness. *Astrophys. J.* **829**, 97. DOI.

Jackson, B.V., Hick, P.P., Buffington, A., Yu, H.-S., Bisi, M.M., Tokumaru, M., Zhao, X.: 2015, A determination of the North–South heliospheric magnetic field component from inner corona closed-loop propagation. *Astrophys. J. Lett.* **803**, L1. DOI.

Kamide, Y., Kusano, K.: 2015, No major solar flares but the largest geomagnetic storm in the present solar cycle. *Space Weather* **13**, 365. DOI.

Kataoka, R., Shiota, D., Kilpua, E., Keika, K.: 2015, Pileup accident hypothesis of magnetic storm on 17 March 2015. *Geophys. Res. Lett.* **42**, 5155. DOI.

Liu, Y.D., Luhmann, J.G., Kajdic, P., Kilpua, E.K.J., Lugaz, N., Nitta, N.V., Möstl, C., Lavraud, B., Bale, S.D., Farrugia, C.J., Galvin, A.B.: 2014, Observations of an extreme storm in interplanetary space caused by successive coronal mass ejections. *Nat. Commun.* **5**, 3481. DOI.

Liu, Y., Hu, H., Wang, R., Yang, Z., Zhu, B., Liu, Y.A., Luhmann, J.G., Richardson, J.D.: 2015, Plasma and magnetic field characteristics of solar coronal mass ejections in relation to geomagnetic storm intensity and variability. *Astrophys. J. Lett.* **809**, L34. DOI.

Lugaz, N., Farrugia, C.J., Winslow, R.M., Al-Haddad, N., Kilpua, E.K.J., Riley, P.: 2016, Factors affecting the geoeffectiveness of shocks and sheaths at 1 AU. *J. Geophys. Res.* **121**, 10,861. DOI.

Manoharan, P.K., Maia, D., Johri, A., Induja, M.S.: 2016, Interplanetary consequences of coronal mass ejections events occurred during 18 – 25 June 2015. In: Dorotovic, I., Fischer, C.E., Temmer, M. (eds.) *Ground-Based Solar Observations in the Space Instrumentation Era*, *ASP Conf. Ser.* **504**, 59.

Marubashi, K., Cho, K.-S., Kim, R.-S., Kim, S., Park, S.-H., Ishibashi, H.: 2016, The 17 March 2015 storm: the associated magnetic flux rope structure and the storm development. *Earth Planets Space* **68**, 173. DOI.

Marubashi, K., Cho, K.-S., Ishibashi, H.: 2017, Interplanetary magnetic flux rope as agent connecting solar eruptions and geomagnetic activities. *Solar Phys.*, submitted.

Möstl, C., Amla, K., Hall, J.R., Liewer, P.C., De Jong, E.M., *et al.*: 2014, Connecting speeds, directions and arrival times of 22 coronal mass ejections from the Sun to 1 au. *Astrophys. J.* **787**, 119. DOI.

Möstl, C., Rollett, T., Frahm, R.A., Liu, Y.D., Long, D.M., Colaninno, R.C., Reiss, M.A., Temmer, M., Farrugia, C.J., Posner, A., Dumbović, M., Janvier, M., Démoulin, P., Boakes, P., Devos, A., Kraaikamp, E., Mays, M.L., Vršnak, B.: 2015, Strong coronal channeling and interplanetary evolution of a solar storm up to Earth and Mars. *Nat. Commun.* **6**, 7135. DOI.

Nitta, N.V., Mulligan, T.: 2017, Earth-affecting coronal mass ejections without obvious low coronal signatures. *Solar Phys.* **292**, 125. DOI.

Richardson, I.G., Webb, D.F., Zhang, J., Berdichevsky, D.B., Biesecker, D.A., *et al.*: 2006, Major geomagnetic storms (Dst ≤ -100 nT) generated by corotating interaction regions. *J. Geophys. Res.* **111**, A07S09. DOI.

Reiff, P.H., Daou, A.G., Sazykin, S.Y., Nakamura, R., Hairston, M.R., *et al.*: 2016, Multispacecraft observations and modeling of the 22/23 June 2015 geomagnetic storm. *Geophys. Res. Lett.* **43**, 7311. DOI.

Rodriguez, L., Zhukov, A.N., Cid, C., Cerrato, Y., Saiz, E., *et al.*: 2009, Three frontside full halo coronal mass ejections with a nontypical geomagnetic response. *Space Weather* **7**, S06003. DOI.

Shen, F., Feng, X.S., Wang, Y., Wu, S.T., Song, W.B., Guo, J.P., Zhou, Y.F.: 2011, Three-dimensional MHD simulation of two coronal mass ejections' propagation and interaction using a successive magnetized plasma blobs model. *J. Geophys. Res.* **116**, A09103. DOI.

Shen, F., Shen, C., Zhang, J., Hess, P., Wang, Y., Feng, X., Cheng, H., Yang, Y.: 2014, Evolution of the 12 July 2012 CME from the Sun to the Earth: data-constrained three-dimensional MHD simulations. *J. Geophys. Res.* **119**, 7128. DOI.

Schwenn, R.: 2006, Space weather: the solar perspective. *Living Rev. Solar Phys.* **3**, 2. DOI.

Thernisien, A.F.R., Howard, R.A., Vourlidas, A.: 2006, Modeling of flux rope coronal mass ejections. *Astrophys. J.* **652**, 763. DOI.

Vrsnak, B., Žic, T., Vrbanec, D., Temmer, M., Rollett, T., *et al.*: 2013, Propagation of interplanetary coronal mass ejections: the drag-based model. *Solar Phys.* **285**, 295. DOI.

Wang, Y., Zhou, Z., Shen, C., Liu, R., Wang, S.: 2015, Investigating plasma motion of magnetic clouds at 1 AU through a velocity-modified cylindrical force-free flux rope model. *J. Geophys. Res.* **120**, 1543. DOI.

Wang, Y., Zhang, Q., Liu, J., Shen, C., Shen, F., Yang, Z., Zic, T., Vrsnak, B., Webb, D.F., Liu, R., Wang, S., Zhang, J., Hu, Q., Zhuang, B.: 2016, On the propagation of a geoeffective coronal mass ejection during 15 – 17 March 2015. *J. Geophys. Res.* **121**, 7423. DOI.

Webb, D.F., Howard, T.A., Fry, C.D., Kuchar, T.A., Mizuno, D.R., Johnston, J.C., Jackson, B.V.: 2009, Studying geoeffective interplanetary coronal mass ejections between the Sun and Earth: space weather implications of Solar Mass Ejection Imager observations. *Space Weather* **7**, S05002. DOI.

Wu, C.C., Liou, K., Socker, D.G., Howard, R., Jackson, B.V., Yu, H.S., Hutting, L., Plunkett, S.P.: 2015, The first super geomagnetic storm of solar cycle 24: "The St. Patrick day (17 March 2015)" event. In: *AGU Fall Meeting 2015, SH51A-2433*.

Wu, C.-C., Kan, L., Lepping, R.P., Hutting, L., Plunkett, S., Howard, R.A., Socker, D.: 2016, The first super geomagnetic storm of Solar Cycle 24: "The St. Patrick's day event (17 March 2015)". *Earth Planets Space* **68**, 151. DOI.

Zhang, J., Richardson, I.G., Webb, D.F., Gopalswamy, N., Huttunen, E., Kasper, J.C., Nitta, N.V., Poomvises, W., Thompson, B.J., Wu, C.-C., Yashiro, S., Zhukov, A.N.: 2007, Solar and interplanetary sources of major geomagnetic storms (Dst ≤ -100 nT) during 1996 – 2005. *J. Geophys. Res.* **112**, A10102. DOI.